

1 **Title:** Rapamycin induced hyperglycemia is associated with exacerbated age-related
2 osteoarthritis

3
4 **Authors:** Dennis M. Minton^{1,2}, Christian J. Elliehausen^{1,2}, Martin A. Javors³, Kelly S.
5 Santangelo⁴, Adam R. Konopka^{1,2,5}

6
7 ¹Department of Medicine, University of Wisconsin-Madison; ²Department of Kinesiology,
8 University of Illinois at Urbana-Champaign; ³Departments of Psychiatry and
9 Pharmacology at University of Texas Health, San Antonio; ⁴Department of Microbiology,
10 Immunology, Pathology, Colorado State University; ⁵Geriatric Research, Education, and
11 Clinical Center, William S. Middleton Memorial Veterans Hospital.

12
13 **Running Title:** Off-target effects of rapamycin worsen age-related OA

14
15 **Corresponding Author:**

16 Adam R. Konopka, PhD
17 Department of Medicine, Division of Geriatrics and Gerontology
18 University of Wisconsin-Madison
19 Geriatric Research, Education, and Clinical Center
20 William S. Middleton Memorial Veterans Hospital
21 akonopka@medicine.wisc.edu

22
23
24
25
26
27
28
29
30
31
32
33
34
35
36
37
38
39

40 **Abstract**

41 *Background:* The objective of this study was to determine if mechanistic target of
42 rapamycin (mTOR) inhibition with or without AMP-activated protein kinase (AMPK)
43 activation can protect against primary, age-related OA.

44 *Design:* Dunkin-Hartley guinea pigs develop mild primary OA pathology by 5-months of
45 age that progresses to moderate OA by 8-months of age. At 5-months, guinea pigs
46 sacrificed as young control (n=3) or were fed either a control diet (n=8), a diet enriched
47 with the mTOR-inhibitor rapamycin (Rap, 14ppm, n=8), or Rap with the AMPK-activator
48 metformin (Rap+Met, 1000ppm, n=8) for 12 weeks. Knee joints were evaluated by OARSI
49 scoring, micro-computed tomography, and immunohistochemistry. Glenohumeral
50 articular cartilage was collected for western blotting.

51 *Results:* Rap and Rap+Met treated guinea pigs displayed lower body weight than control.
52 Rap and Rap+Met inhibited articular cartilage mTORC1 but not mTORC2 signaling.
53 Rap+Met, but not Rap alone, stimulated AMPK. Despite lower body weight and articular
54 cartilage mTORC1 inhibition, Rap and Rap+Met treated guinea pigs had greater OA
55 severity in the medial tibial plateau due to articular cartilage structural damage and/or
56 proteoglycan loss. Rap and Rap+Met increased plasma glucose compared to control.
57 Plasma glucose concentration was positively correlated with proteoglycan loss,
58 suggesting hyperglycemic stress may have contributed to worsened OA.

59 *Conclusions:* This is the first study to show that Rap induced increase in plasma glucose
60 was associated with greater OA severity. Further, articular cartilage mTORC1 inhibition
61 and bodyweight reduction by dietary Rap and Rap+Met did not protect against primary
62 OA during the prevailing hyperglycemia.

63 **Key Words:** Aging, mTOR, AMPK, Dunkin Hartley Guinea Pig, Primary Osteoarthritis

64 **Background**

65 Primary, age-related osteoarthritis (OA) is estimated to account for as many as 90%
66 of all knee OA cases in humans (1). However, preclinical research commonly relies on
67 experimental models of secondary OA. Although primary and secondary OA share similar
68 pathological outcomes, there is a growing body of evidence to suggest they are driven by
69 distinct mechanisms. Retrospective analysis of differentially expressed genes from
70 separate cohorts of primary and secondary OA patients relative to their healthy controls
71 found that only 10% of differentially upregulated and 35% of differentially downregulated
72 genes in OA vs non-OA samples are conserved between primary and secondary OA
73 (2,3). Therefore, 65-90% of differentially expressed genes may be unique to primary
74 versus secondary OA. Additionally, transgenic animal models have revealed that several
75 genes are differentially involved in the progression of primary and secondary OA (4–9).
76 For example, deletion of *Panx3* protects against secondary OA yet dramatically worsens
77 primary OA (4), and deletion of *JNK1/2* accelerates the development of primary OA while
78 having no effect on secondary OA progression (9). Together, these studies reinforce that
79 unique mechanisms underpin these two forms of OA.

80 Age is one of the greatest risk factors for nearly every chronic disease, including
81 primary OA. Two evolutionarily conserved kinases, mechanistic target of rapamycin
82 (mTOR) and AMP-activated protein kinase (AMPK), are energy sensing pathways
83 similarly dysregulated during aging and OA (10–13). The mTOR inhibitor rapamycin (Rap)
84 can extend lifespan in mice and delay the onset of several age-related morbidities (12,14).
85 The anti-diabetic drug metformin (Met) can activate AMPK and, when added to Rap,
86 extends lifespan to a greater extent than historical cohorts of mice treated with Met or

87 Rap alone (15). Additionally, Met is the first drug being tested to slow age-related multi-
88 morbidity in humans (16). While the prospect of lifespan extension is tantalizing,
89 extending lifespan without delaying the onset or slowing the progression of the most
90 debilitating age-associated conditions could be viewed as detrimental. Therefore, it is
91 imperative to understand if purported lifespan-extending therapies that target the
92 fundamental biology of aging are also capable of delaying the onset of chronic diseases,
93 such as primary OA.

94 mTOR exists as complex I (mTORC1) and complex II (mTORC2). mTORC1 regulates
95 cellular proliferation, protein synthesis, senescence, and survival while mTORC2
96 functions downstream of insulin signaling on substrates such as PI3K-Akt (12). In articular
97 cartilage, mTORC1 activity increases with age and is sufficient to induce OA in young
98 male mice (10). In non-articular tissues, acute or intermittent Rap selectively inhibits
99 mTORC1 while chronic Rap administration for durations greater than 14 days also inhibits
100 mTORC2 activity (17). Cartilage-specific deletion of mTOR and systemic or intra-articular
101 injections of Rap and the mTORC1/2 inhibitor Torin 1 lower secondary OA in young-male
102 mice and rabbits (18–21). While these findings support mTOR-based therapeutics for OA,
103 the completed studies were exclusively in injury-induced models of OA and have not been
104 investigated in primary, age-related OA.

105 Recently, it has been proposed that the positive effects of mTOR inhibition on OA
106 pathology may be diminished by feedback activation of PI3K and has raised questions
107 about the need for a dual treatment strategy that inhibits both mTOR and upstream PI3K
108 signaling (22,23). In addition to activating AMPK, Met has pleotropic effects including
109 inhibition of PI3K signaling in rheumatoid arthritis fibroblast-like synoviocytes (24).

110 Moreover, Met and other AMPK-activators have chondroprotective effects against
111 inflammatory-induced protease expression *in vitro* (25,26) and protect against injury-
112 induced OA in young male mice and rhesus monkeys (27). Treatment with Met is also is
113 associated with a lower rate of medial tibiofemoral cartilage volume loss and risk of total
114 knee replacement in obese patients (28). However, Met as an adjuvant therapy to Rap
115 has not been investigated in primary OA.

116 The Dunkin-Hartley guinea pig is a well-characterized outbred model of primary OA.
117 The progression of OA in guinea pigs is related to bodyweight (29) and shares a similar
118 age-related and spatial progression to humans (30). Mild OA pathology develops by 5
119 months in guinea pigs that progresses to moderate OA by 8-9 months of age (30–32).
120 Therefore, at 5 months of age we treated guinea pigs with lifespan-extending doses of
121 Rap or a combination of Rap+Met for 12 weeks to slow the progression from mild to
122 moderate OA. This study is the first to evaluate if lifespan extending treatments can
123 modify primary OA, the most prevalent form of OA observed in older adults.

124 **Methods**

125 Animal Use

126 All tissues were collected at the University of Illinois Urbana-Champaign and
127 approved by the Institutional Animal Care and Use Committee. Data collection and
128 analysis were completed at University of Wisconsin-Madison and William S. Middleton
129 Memorial Veterans Hospital. Because male Dunkin-Hartley guinea pigs develop more
130 severe OA pathology than female (33), we used male animals to maximize the potential
131 for the interventions to slow the progression of OA. Therefore, similar to previous work
132 (34), male Dunkin-Hartley guinea pigs (Charles River) were singly housed in clear plastic,
133 flat bottomed cages (Thoren, Model #6) with bedding. Guinea pigs were single housed to
134 measure food consumption. 12-hour light/dark cycles were used beginning at 0600.
135 Guinea pigs acclimated for 2-3 weeks and were provided standard chow diet (Evigo 2040)
136 fortified with vitamin C (1050 ppm) and Vitamin D (1.5 IU/kg) and water ad libitum until 5
137 months of age. Guinea pigs were then sacrificed to serve as young control (n=3),
138 randomized to continue the standard diet (n=8), or receive standard diets enriched with
139 encapsulated rapamycin (14 ppm, n=8) or the combination of encapsulated rapamycin
140 and metformin (14 ppm, 1000 ppm, n=8) for 12 weeks. Guinea pigs were randomized to
141 match bodyweight between groups prior to beginning treatment. Diets were enriched with
142 microencapsulated rapamycin (Rapamycin holdings) and/or metformin (AK Scientific,
143 I506) at concentrations previously shown to extend lifespan in mice (14,15,35). Food
144 consumption was recorded on Monday, Wednesday, and Friday between 8 and 9 AM,
145 and body weight was recorded before feeding on Monday. Guinea pigs treated with Rap
146 or Rap+Met diet had ad libitum access to food. Dietary Rap treatment has been shown to

147 significantly reduce bodyweight in mice (36,37). Therefore, we matched food
148 consumption in the control group to the Rap diets to minimize the influence of food intake
149 on dependent variables. One guinea pig in the Rap+Met group was euthanized early due
150 to a wound on the gums which led to suppressed appetite and infection. Tissues from this
151 animal were not collected for analysis. It could not be determined if this was due to a
152 laceration or an oral ulcer, the latter of which is a known side effect of mTOR inhibitors
153 (38).

154

155 Tissue Collection

156 Two animals were sacrificed daily between 7 and 10 AM. Food and water were
157 removed from the cages 2-4 hours before euthanasia. Animals were anesthetized in a
158 chamber containing 5% isoflurane gas in oxygen and maintained using a face mask with
159 1.5-3% isoflurane. Blood was collected by cardiac venipuncture followed by excision of
160 the heart. The right hind limb was removed at the coxofemoral joint, fixed in 10% neutral
161 buffered formalin (NBF) for 48 hours, and transferred to 70% ethanol until processed for
162 histology. Glenohumeral cartilage was collected, snap frozen in liquid nitrogen, and stored
163 at -80C for further analysis. Because testicular atrophy has been observed following Rap
164 treatment (39), the left testicle was preserved in 10% NBF and weighed. Although tissues
165 are commonly weighed before fixation, previous work demonstrates that fixation
166 negligibly effects testicle weight in similarly sized rodents (40).

167

168

169

170 Analysis of Experimental Diets and Blood

171 Samples of diets enriched with Rap, Met or the combination of Rap+Met, and
172 aliquots of whole blood (n=4 per group) were sent to the Bioanalytical Pharmacology Core
173 at the San Antonio Nathan Shock Center to confirm drug concentrations in the diet and
174 in circulation. Analysis was performed using tandem HPLC-MS as described previously
175 (14,41,42). Frozen aliquots of plasma were thawed to measure glucose and lactate
176 concentrations using the YSI Biochemistry Analyzer (YSI 2900).

177

178 Micro Computed Tomography (μ CT)

179 Right hind limbs from half of each treatment group (n=4 per group) were scanned
180 using a Rigaku CT Lab GX130 at 120 μ A and 110 kV for 14 minutes, achieving a pixel
181 size of 49 μ m. Scans were first processed in Amira 6.7 (ThermoFisher) where epicondylar
182 width was measured and a series of dilation, erosion, filling, and image subtraction
183 functions were used to isolate trabecular and cortical bone as described previously (43).
184 Scans were then resliced 4 times along axes perpendicular to medial and lateral tibial
185 and femoral articular surfaces and binarized using identical thresholds. NIH ImageJ
186 software and BoneJ plugin were used to quantify thickness, spacing, and volume fraction
187 measurements. Cortical thickness was measured by placing polygonal regions of interest
188 (ROI) in resliced scans to encompass the articular surfaces in each joint compartment.
189 Trabecular thickness, spacing, and bone volume fraction were measured by placing
190 transverse ROIs (2.4x2.4x1mm) in the trabecular bone of each joint compartment.

191

192

193 Histology

194 Knee joints were decalcified in a 5% ethylenediaminetetraacetic acid, changed every 2-
195 3 days for 6 weeks. Joints were then cut in a coronal plane along the medial collateral
196 ligament, paraffin embedded and sectioned at 5um increments for Toluidine Blue
197 staining and immunohistochemistry (IHC). Slides were scanned using the Hamamatsu
198 NanoZoomer Digital Pathology System, providing 460nm resolution. Scan focus points
199 were set manually along the articular cartilage. Imaged slides were then scored by two
200 blinded reviewers for OA severity following OARSI Modified Mankin guidelines as
201 described (32). Briefly, toluidine blue stained histology slides were assigned scores for
202 severity of articular cartilage structural damage (0-8), proteoglycan loss as assessed by
203 absence of toluidine blue staining (0-6), disruption of chondrocyte cellularity (0-3), and
204 tidemark integrity (0-1), with a total possible score of 18 per joint compartment (Total
205 OARSI Score). One guinea pig each from the Rap and Met groups were unable to be
206 analyzed due to off-axis transection before embedding. One control animal was a
207 statistical outlier as detected by Grubb's test and was excluded from the study.
208 Therefore, n=7 per group were used for histopathological analysis.

209

210 Immunohistochemistry

211 Antigen retrieval was performed in 10mM sodium citrate for 7 hours at 60C.
212 Endogenous peroxidase activity was quenched using 3% H₂O₂ for 15min before blocking
213 in 5% normal goat serum diluted in TBST for 1 hour at RT. Slides were incubated
214 overnight in 200-300 uL of either p-RPS6 (1:200 dilution; Cell Signaling, 4858) or a rabbit
215 IgG isotype control (Cell Signaling, 3900) diluted to match primary antibody concentration.

216 Primary antibodies against p-Akt Ser473 (1:100 dilution; 4060) and p-AMPK Thr172
217 (1:200 dilution; 50081) from Cell Signaling were attempted, but reactivity was not seen in
218 guinea pig articular cartilage. 150-200uL of goat anti-rabbit secondary antibody (Cell
219 Signaling, 8114) was added for 1 hour at room temperature followed by exposure in 3,3'-
220 diaminobenzidine (DAB; Cell Signaling, 8059) for 10 minutes. Slides were then
221 counterstained using hematoxylin, dehydrated, and cleared through graded ethanol and
222 xylene, coverslipped using Permount (Electron Microscopy Sciences), and viewed and
223 imaged under a brightfield microscope. No DAB staining was seen following incubation
224 with the IgG control or secondary antibody alone, confirming specificity of the primary
225 antibody. For quantification, ROIs were placed to encompass areas of staining in the
226 medial tibial articular cartilage, and cells were counted to determine the percent-positive
227 cells. For intensity-based quantification, a color deconvolution for DAB staining was
228 applied in ImageJ, and mean integrated intensity was quantified by averaging two p-RPS6
229 replicates and subtracting background staining of IgG controls.

230

231 Western Blot

232 Cartilage was removed from the glenohumeral joint using a scalpel and placed in
233 reinforced Eppendorf tubes containing 500 mg of ceramic beads (Fisher, 15-340-160)
234 and 200 μ L of RIPA buffer with protease and phosphatase inhibitors (Sigma,
235 5892970001), and homogenized by 2, 30-second cycles at 6 m/s in the Omni
236 BeadRuptor. Homogenate was transferred to microcentrifuge tubes and spun at 10,000g
237 for 10 min at 4C. Supernatants were diluted to equal concentration following a BCA assay.
238 Samples were prepared in reducing conditions with β -mercaptoethanol in 4x Laemmli

239 Sample Buffer (BioRad, 1610747) and heated at 95C for 5 minutes. 10 µg of protein was
240 separated on 4-15% TGX precast gels (BioRad, 4561083) and transferred to PVDF
241 membranes (BioRad, 1620177). Membranes were blocked in TBST with 5% bovine
242 serum albumin (Sigma, A9647) for 1 hour at RT and incubated overnight at 4C in primary
243 antibodies against p-RPS6 Ser235/236 (4858), RPS6 (2217) p-Akt Ser473 (4060), Akt
244 (4685), P-AMPK Thr172 (50081), AMPK (2532), and LC3B (3868) from Cell Signaling
245 and ADAMTS5 (ab41037), MMP-13 (ab39012), and b-Actin (ab8226) from Abcam. HRP-
246 conjugated anti-Rabbit (Cell Signaling) or anti-Mouse (Abcam) secondary antibodies
247 were diluted 1:5,000 for all proteins except b-Actin (1:10,000 dilution). All membranes
248 were imaged using a UVP BioSpectrum 500 (UVP) following 5-minute incubation in a 2:1
249 combination of SuperSignal Pico (Fisher, 34577) and Femto (Fisher, PI34095)
250 chemiluminescent substrates except b-Actin which received Pico alone. Densitometric
251 analysis was performed using VisionWorks (Analytikjena). Phosphorylated proteins are
252 expressed relative to their total protein and other targets are expressed relative to b-Actin.
253

254 **Statistical Analysis**

255 Previous work demonstrated that a sample size of n=6 is adequately powered to
256 detect changes between groups in guinea pigs (34). Therefore, we a priori determined
257 our sample size (n=7-8 per group) to be appropriate to detect differences between
258 treatment groups. All data were subjected to normality testing via the Shapiro-Wilk test.
259 Comparisons of normally distributed data were performed using two-way unpaired t-tests
260 or one-way ANOVA followed by Holm-Sidak's multiple comparison test. Data with non-
261 Gaussian distribution were compared using non-parametric Mann-Whitney tests or the

262 Kruskal-Wallis test followed by Dunn's multiple comparisons test. A two-way repeated
263 measures ANOVA (time x treatment) was performed to determine differences in food
264 consumption and body weight. Upon a significant interaction, Holm-Sidak's multiple
265 comparisons test was used. Because we were interested in determining if treatments
266 impacted the trajectory of OA pathogenesis compared to aged controls, differences in all
267 other variables besides plasma glucose were made using one-way ANOVA comparing
268 treatment groups to 8-month controls. Due to previous reports that Met can rescue the
269 hyperglycemic effects of Rap (37), comparisons were made between all groups for
270 plasma glucose. Pearson's R was used to determine correlation between variables. P-
271 values <0.05 were considered statistically significant. Data are presented as scatter plots
272 with mean or mean \pm standard deviation (SD).

273

274

275

276

277

278

279 **Results**

280 *Influence of rapamycin and rapamycin+metformin on guinea pig physical and metabolic*
281 *characteristics*

282 Figure 1A shows the average daily food consumption per week of standard diet or
283 standard diet enriched with Rap or Rap+Met. The average daily intakes of Rap and Met
284 based on food consumption and dietary concentration are reported in Table 1. Compared
285 to control, there was decreased food consumption in guinea pigs receiving Rap+Met
286 during week 2 ($P=0.04$). There were no significant differences between
287 treatments. Despite largely matching food intake, there was a significant effect for
288 treatment ($P=0.004$) and an interaction between time and treatment ($P<0.0001$) on
289 bodyweight. Rap+Met ($P=0.01$) and Rap-treated guinea pigs ($P=0.02$) were smaller than
290 control starting at week 3 and week 4, respectively, until the end of the study (Figure 1B).
291 At sacrifice, Rap ($P=0.002$) and Rap+Met-treated guinea pigs ($P=0.001$) were 15% and
292 22% smaller than control.

293 Treatment with Rap (396 ± 61 mg/dL; $P<0.0001$) and Rap+Met (334 ± 53 mg/dL;
294 $P=0.007$) increased plasma glucose compared to control (234 ± 55 mg/dL), and the
295 addition of Met to Rap decreased plasma glucose compared to Rap alone ($P=0.05$; Figure
296 1C). Lactate concentration tended to be elevated by 66% in Rap+Met-treated guinea
297 pigs, only ($P=0.07$; Figure 1D). Testicle weight in guinea pigs receiving Rap ($P=0.006$)
298 and Rap+Met ($P=0.0003$) were 27% and 44% lower than control, respectively, suggesting
299 gonadal atrophy (Figure 1E). We analyzed blood for the circulating Rap and Met
300 concentrations ~3-hours after food had been removed from the cage (Table 2). This
301 timing aligns with a measurement of peak circulating Rap and Met. We saw that

302 experimental diets were sufficient to increase Rap and Met concentrations in the blood,
303 and that Rap values were not different when providing diets individually or in combination.
304 There was no Rap or Met detected in circulation in control animals.

305
306 *Rapamycin and rapamycin+metformin treatment exacerbated the age-related*
307 *progression of OA*

308 Consistent with the age-related progression of mild to moderate OA in guinea pigs,
309 we observed an increase in medial tibial total OARSI score from 5 to 8 months ($P=0.03$;
310 Figure S1A-B). Surprisingly, Rap and Rap+Met treatment resulted in a ~2-fold increase
311 in total OARSI score in the medial tibial plateau compared to 8 month old, age-matched
312 control ($P=0.02$ for both Rap and Rap+Met; Figure 2B). This was driven by increased
313 scores for articular cartilage structure ($P=0.02$ for Rap, $P=0.11$ for Rap+Met; Figure 2C)
314 and proteoglycan loss ($P=0.02$ for Rap and Rap+Met; Figure 2D). There was no
315 significant effect of Rap or Rap+Met on the OARSI score for the lateral tibia or medial or
316 lateral femur (Figure S1C).

317
318 *OA pathology was correlated to plasma glucose, bodyweight, and testicle weight*

319 Because Rap and Rap+Met treated guinea pigs displayed several side effects of
320 Rap, including increased plasma glucose, testicular atrophy, decreased bodyweight, and
321 worsened OA pathology, we evaluated the relationship between these variables and
322 measures of OA severity across all guinea pigs. Plasma glucose was positively correlated
323 to proteoglycan loss ($R^2=0.19$; $P=0.04$; Figure 3A), and total OARSI score was negatively
324 correlated with both bodyweight ($R^2=0.19$; $P=0.04$; Figure 3B) and testicle weight

325 (R²=0.20; P=0.04; Figure 3C). However, because testicle weight and bodyweight were
326 also related (data not shown), the individual contribution of these variables cannot be
327 resolved.

328

329 *Effects of rapamycin and rapamycin+metformin on mTOR, AMPK, and protease*
330 *expression*

331 To evaluate mTORC1 signaling in articular cartilage, we measured the
332 phosphorylation of ribosomal protein S6 (P-RPS6) at Ser235/236 using IHC and western
333 blotting. Representative images of P-RPS6 IHC are shown in Figure 4A. P-RPS6 was
334 decreased by 90-95% in the medial tibial articular cartilage of Rap and Rap+Met treated
335 guinea pigs as assessed by percentage of P-RPS6-positive cells (P=0.001 for Rap,
336 P=0.01 for Rap+Met; Figure 4B), and by staining intensity (P=0.02 for both; Figure 4C).
337 mTORC1 inhibition was further supported by an 81% lower ratio of phosphorylated to
338 total RPS6 in glenohumeral cartilage from Rap (P=0.005; Figure 4E). Rap+Met trended
339 to decrease RPS6 phosphorylation by 48% (P=0.06). There were no significant effect on
340 the phosphorylation of the mTORC2 substrate Akt at Ser473 in Rap or Rap+Met
341 compared to control (Figure 4F; P=0.11). AMPK activity was measured using western blot
342 to assess phosphorylation of AMPK at Thr172 (P-AMPK). P-AMPK was not changed by
343 Rap alone (P=0.83; Figure 4G) but was elevated 77% by Rap+Met (P=0.05). Rap or
344 Rap+Met did not significantly change the conversion of LC3B I to II (P>0.99 for both;
345 Figure 4H) nor a disintegrin and metalloproteinase with thrombospondin motifs 5
346 (ADAMTS5; Figure 4I; P=0.97 for Rap, P=0.35 for Rap+Met). Matrix metalloproteinase

347 13 (MMP13) was unchanged by Rap ($P>0.99$) but trended higher in Rap+Met ($P=0.09$;
348 Figure 4J).

349
350 *Rapamycin and rapamycin+metformin decreased subchondral and diaphyseal bone*
351 *thickness*

352 Representative microCT images shown in Figure 5A were used to quantify the
353 effect of experimental diets on subchondral bone parameters. Mean subchondral cortical
354 thickness was decreased by Rap and Rap+Met in the medial (29%, $P=0.003$ for Rap;
355 23%, $P=0.007$ for Rap+Met) and lateral (21% for Rap; 20% for Rap+Met; $P=0.01$ for both)
356 tibia (Figure 5B). Rap and Rap+Met decreased trabecular spacing by 15% and 16%,
357 respectively, in the lateral tibia only ($P=0.006$ for both; Figure S2B). Trabecular thickness,
358 trabecular spacing in other compartments, and bone volume fraction were not affected by
359 any experimental diet (Figures S2A-C). Further investigation revealed that cortical
360 thickness at the femoral diaphysis was decreased by Rap ($P=0.001$) and Rap+Met
361 ($P=0.01$; Fig 5C), and this change was proportionate to the decrease observed in the
362 medial tibial subchondral bone (Figure 5D). Further, medial tibial cortical thickness was
363 correlated to bodyweight ($R^2=0.47$, $P=0.01$; Figure 5E), suggesting the smaller body
364 mass of Rap and Rap+Met treated guinea pigs may have contributed to decreased
365 cortical thickness. Femoral epicondylar width (Figure 5F) was not statistically different
366 between groups (Rap, $P=0.42$; Rap+Met, $P=0.45$), suggesting our treatments did not
367 affect skeletal development.

368
369

370 **Discussion**

371 The purpose of this study was to test if dietary Rap or Rap+Met could delay the
372 onset of age-related OA in the outbred Dunkin-Hartley guinea pig. We found that at
373 concentrations shown to extend lifespan, dietary Rap and Rap+Met inhibited mTORC1
374 but not mTORC2 signaling in articular cartilage, and Rap+Met increased AMPK
375 phosphorylation. Surprisingly, guinea pigs treated with Rap, with or without Met,
376 developed greater age-related OA compared to control. Guinea pigs receiving Rap and
377 Rap+Met also displayed increased plasma glucose, which correlated with proteoglycan
378 loss. These findings indicate that off-target side effects of Rap are associated with greater
379 OA pathology. Further, in the face of these Rap-induced side effects, mTORC1 inhibition
380 may not slow the progression of age-related OA in Dunkin Hartley guinea pigs.

381 Despite inhibiting mTORC1 in articular cartilage, our findings indicate that guinea
382 pigs treated with Rap, with or without Met, had exacerbated age-related OA in the medial
383 tibial plateau. Further, Rap and Rap+Met treated guinea pigs had greater total OARSI
384 scores even though they weighed less, which is contrary to previous work where lower
385 body weight was accompanied by lower OA scores in guinea pigs (29). Although there is
386 precedent that mTORC1 inhibition by intra-articular injection of Rap is associated with
387 exacerbated temporomandibular joint (TMJ) OA (44), our findings were opposite of our
388 original hypothesis and previous results using Rap in secondary models of knee OA
389 (18,19). The guinea pigs in the current study received a dose of Rap that achieved similar
390 circulating Rap concentrations shown to extend lifespan in mice (14). Additionally, the
391 dose of Rap in guinea pigs was similar to the dose shown to protect against secondary
392 OA in mice (0.7 vs 1 mg/kg/day in guinea pigs vs. mice) (18). These findings suggest that

393 dose of Rap was not a likely factor contributing to differences between studies. In our
394 study, Rap and Rap+Met treatment inhibited mTORC1 but not mTORC2 in articular
395 cartilage. Previous work has shown that deleting articular cartilage mTOR (21) or treating
396 with Rap (18,19) or Torin-1 (20) can attenuate secondary OA in mice and rabbits. These
397 non-selective genetic and pharmacological methods likely disrupt the entire mTOR kinase
398 and therefore could inhibit both mTORC1 and mTORC2 signaling. However, this remains
399 speculative as mTORC2 signaling was not evaluated in these previous studies, and it
400 continues to be unknown if mTORC2 inhibition is necessary for protection against either
401 primary or secondary OA. In support of the notion that targeting mTORC2 modifies OA,
402 inhibition of the mTORC2 substrate Akt protects against PTEN-deletion-induced OA by
403 decreasing cellular senescence and oxidative stress (45). Further investigation is needed
404 to resolve the role of each mTOR complex in the initiation, progression, and treatment of
405 both primary and secondary OA.

406 Despite its lifespan-extending effects, chronic Rap treatment is commonly
407 associated with several metabolic and immunological side effects including glucose
408 intolerance, insulin resistance, hypertriglyceridemia, immunosuppression, testicular
409 atrophy, lower body weight, and cataracts (17,39,46). Consistent with this, we showed
410 that 12-weeks of dietary Rap and Rap+Met was accompanied by increased plasma
411 glucose, testicular atrophy, and lower body weight. Despite increasing AMPK activity in
412 articular cartilage and partially restoring glucose levels compared to Rap alone, the
413 addition of Met to Rap did not offer protection against the detrimental effects of dietary
414 Rap on OA pathology. The glucose lowering effects of Met are in line with previous studies
415 where Met alleviated Rap-induced glucose intolerance only in female mice (37).

416 However, our OA pathology findings are in contrast to previous studies that showed Met
417 attenuated hyperglycemia-induced OA in mice (55). In our study, medial tibial
418 proteoglycan loss was correlated with plasma glucose, and we propose that Rap-induced
419 hyperglycemia may have contributed to worsened OA following dietary Rap treatment. In
420 support of this hypothesis, diabetic mice show accelerated OA after injury, and
421 chondrocytes cultured in high glucose media display decreased expression of Collagen
422 II and increased MMP13 and inflammatory mediators IL-6 and NFkB (47,48). However,
423 intermittent intraperitoneal injections of Rap lowered glucose and mitigated diabetes
424 accelerated secondary OA (49). It is possible that Rap did offer partial protection against
425 hyperglycemic stress but still resulted in greater OA pathology than control, as was
426 observed by Ribeiro et al. (50). However, this remains speculative as we did not have a
427 group exposed to hyperglycemic stress alone. Previous work suggests Rap can have
428 divergent effects where it is beneficial in some diabetic models but causes adverse side
429 effects in metabolically healthy models (17,51). Collectively, these data indicate that the
430 adverse metabolic side-effects of dietary Rap treatment are associated with a deleterious
431 impact on primary OA pathology and could limit the utility of systemic Rap as a healthspan
432 extending treatment.

433 Rap has been implicated in attenuating secondary OA by increasing autophagy
434 and decreasing protease expression (18,19). While autophagy is a highly dynamic
435 process, the static marker of autophagy, LC3B, is commonly used as a surrogate for
436 autophagic flux. In our study, we saw no effect by any treatment on LC3B or ADAMTS5,
437 while Rap+Met trended to increase MMP13 in glenohumeral cartilage. Therefore, the
438 inability to increase markers of autophagy and decrease proteases may be one

439 contributing factor to why our lifespan-extending treatments did not protect and even
440 worsened OA during aging and hyperglycemia. However, because proteoglycan loss was
441 observed independent of increased protease expression in Rap-treated guinea pigs,
442 decreased extracellular matrix (ECM) protein synthesis may have contributed to
443 proteoglycan loss. More work is needed to determine the molecular and cellular
444 mechanisms responsible for the deleterious effects of Rap and Rap+Met.

445 Treatment with Rap and Rap+Met also decreased subchondral cortical bone
446 thickness in the medial and lateral tibia and the femoral diaphysis. As bone growth in
447 guinea pigs ceases by 4 months (52), and epicondylar width was not different between
448 groups, the differences in bone thickness were likely not the result of disrupted
449 development. Decreased subchondral thickness was only observed in the tibia. Intra-
450 articular injection of Rap into the TMJ caused subchondral bone loss by inhibiting pre-
451 osteoblast proliferation (44), and Rap treatment also decreased osteoblast differentiation
452 and bone matrix synthesis (53), which supports the idea that Rap can act directly on the
453 bone to decrease thickness. However, we also found that subchondral thickness was
454 highly correlated to bodyweight. This is in line with Wolff's law and agrees with previous
455 findings where bodyweight restriction decreased cortical bone thickness in the femoral
456 diaphysis (54). Therefore, both local and systemic effects of Rap likely contributed to
457 reduced cortical bone thickness.

458 Although we provide new insight into the role of mTOR during primary OA
459 progression, we recognize some study limitations. While the guinea pig is an excellent
460 model of primary OA, it is not a widespread model for biomedical research and molecular
461 probes are seldom designed for reactivity with guinea pig tissue. Due to reactivity issues

462 with IHC in guinea pig cartilage (Figure S3), some of our analyses relied on western blot
463 from glenohumeral cartilage. Although guinea pigs also develop mild glenohumeral
464 OA(30), this is not the site at which we measured OA pathology. Our study could not
465 conclusively determine if the deleterious effects of Rap stemmed from its direct effects on
466 the joint or off-target effects on other tissues. However, our data suggest hyperglycemia
467 induced by off-target actions of Rap was associated with worsened age-related OA. The
468 Dunkin Hartley guinea pig is an outbred model of primary OA which leads to inherent
469 variability. While this could be perceived as a limitation, we contend that the variability
470 and the choice of animal model adds translational value since this more closely
471 recapitulates the genetic diversity and OA heterogeneity in humans. We acknowledge
472 that although the sample size used in our study was in line with previous studies using
473 guinea pigs, the variability could have possibly limited our ability to detect more subtle
474 differences between groups. However, this does not detract from the findings that guinea
475 pigs treated with both Rap and Rap+Met had worse OA. Further, the presence of largely
476 overlapping and consistent deleterious outcomes in both groups receiving Rap increases
477 our confidence that the side effects accompanying Rap contribute to worsened primary
478 OA.

479

480 **Conclusion**

481 In summary, we have shown that at doses previously shown to extend lifespan, dietary
482 Rap and Rap+Met caused hyperglycemia and was associated with aggravated OA in
483 Dunkin Hartley guinea pigs despite inhibiting mTORC1 in articular cartilage. Treatments
484 that extend lifespan without a proportional delay in age-related chronic diseases and

485 disabilities is counter to the concept of healthspan extension. Our findings that guinea
486 pigs treated with Rap had worse OA pathology raises concerns regarding the efficacy of
487 dietary Rap as a life- and healthspan-extending agent. Additional work is needed to
488 investigate the role of alternative routes of administration or Rap anaologs that may
489 capture the positive benefits of Rap while minimizing off-target effects. Our data also
490 reveal that the contribution of mTOR in articular cartilage and chondrocyte metabolism is
491 incompletely understood and additional research is needed to clarify the individual and
492 combined role of mTORC1 and mTORC2 signaling in both primary and secondary OA.

493

494 **Abbreviations**

495 OA: osteoarthritis; mTOR: mechanistic target of rapamycin; AMPK: AMP-activated
496 protein kinase; Rap: rapamycin; Met: metformin; mTORC1: mTOR complex I; mTORC2:
497 mTOR complex II; NBF: neutral buffered formalin; μ CT: micro computed tomography;
498 ROI: region of interest; IHC: immunohistochemistry; OARSI: osteoarthritis research
499 society international; SD: standard deviation; RPS6: ribosomal protein S6; ADAMTS5: a
500 disintegrin and metalloproteinase with thrombospondin motifs 5; MMP13: matrix
501 metalloproteinase 13; TMJ: temporomandibular joint; IL-6: interleukin 6; NFkB: nuclear
502 factor kappa-light-chain-enhancer of activated B-cells; ECM: extracellular matrix.

503

504 **Acknowledgements**

505 The authors would like to thank Greg Friesenhahn at the Analytical Pharmacology and
506 Drug Evaluation Core of the San Antonio Nathan Shock Center. We would also like to
507 acknowledge the technical assistance from William Fairfield, Oscar Safairad, Alex Nichol,

508 Nathan Carper, and Morgan Berland. We also acknowledge the assistance of the
509 University of Wisconsin Translational Research Initiatives in Pathology (TRIP) laboratory
510 supported by the UW Department of Pathology and Laboratory Medicine, UWCCC (P30
511 CA014520).

512

513 **Author Contributions**

514 Study design: AK. Data collection: DM, CE, AK, KS, MJ. Data analysis and
515 interpretation: DM, AK. Manuscript preparation: DM, AK. All authors approved of the
516 final manuscript.

517

518 **Funding**

519 The Konopka Laboratory was supported by the Campus Research Board at the University
520 of Illinois and startup funds from the University of Wisconsin-Madison School of Medicine
521 and Public Health, Department of Medicine, and National Institutes of Health grant R21
522 AG067464. This work was supported using facilities and resources from the William S.
523 Middleton Memorial Veterans Hospital. The content is solely the responsibility of the
524 authors and does not necessarily represent the official views of the NIH, the Department
525 of Veterans Affairs, or the United States Government.

526

527 **Availability of Data and Materials**

528 Data from this study are available from the corresponding author upon reasonable
529 request.

530

531 **Ethics Approval**

532 Animal use was approved by the University of Illinois at Urbana-Champaign IRB and
533 IACUC.

534

535 **Consent for Publication**

536 Not applicable.

537

538 **Competing Interests**

539 The authors have no competing interests to disclose.

540

541 **References**

- 543 1. Brown TD, Johnston RC, Saltzman CL, Marsh JL, Buckwalter JA. Posttraumatic
544 Osteoarthritis: A First Estimate of Incidence, Prevalence, and Burden of Disease.
545 *J Orthop Trauma*. 2006 Nov;20(10):739–44. Available from:
546 <https://pubmed.ncbi.nlm.nih.gov/17106388/>
- 547 2. Aki T, Hashimoto K, Ogasawara M, Itoi E. A whole-genome transcriptome
548 analysis of articular chondrocytes in secondary osteoarthritis of the hip. Agarwal
549 S, editor. *PLoS One*. 2018 Jun 26;13(6):e0199734. Available from:
550 <https://pubmed.ncbi.nlm.nih.gov/29944724/>
- 551 3. Xu Y, Barter MJ, Swan DC, Rankin KS, Rowan AD, Santibanez-Koref M, et al.
552 Identification of the pathogenic pathways in osteoarthritic hip cartilage:
553 commonality and discord between hip and knee OA. *Osteoarthr Cartil*. 2012
554 Sep;20(9):1029–38. Available from: <https://pubmed.ncbi.nlm.nih.gov/22659600/>
- 555 4. Moon PM, Shao ZY, Wambiekele G, Appleton CTG, Laird DW, Penuela S, et al.
556 Global Deletion of Pannexin 3 Resulting in Accelerated Development of Aging-
557 Induced Osteoarthritis in Mice. *Arthritis Rheumatol*. 2021 May 25; Available from:
558 <https://pubmed.ncbi.nlm.nih.gov/33426805/>
- 559 5. Yu D, Hu J, Sheng Z, Fu G, Wang Y, Chen Y, et al. Dual roles of misshapen/NIK-
560 related kinase (MINK1) in osteoarthritis subtypes through the activation of TGF β
561 signaling. *Osteoarthr Cartil*. 2020 Jan;28(1):112–21. Available from:
562 <https://pubmed.ncbi.nlm.nih.gov/31647983/>
- 563 6. Boudreuil T, Vuppalapati KK, Newton PT, Li L, Barenjius B, Chagin AS.
564 Targeted deletion of Atg5 in chondrocytes promotes age-related osteoarthritis.
565 *Ann Rheum Dis*. 2016 Mar;75(3):627–31. Available from:
566 <https://pubmed.ncbi.nlm.nih.gov/26438374/>

567 7. O'Conor CJ, Ramalingam S, Zelenski NA, Benefield HC, Rigo I, Little D, et al.
568 Cartilage-specific knockout of the mechanosensory ion channel TRPV4
569 decreases age-related osteoarthritis. *Sci Rep.* 2016;6(July):1–10. Available from:
570 <http://dx.doi.org/10.1038/srep29053>

571 8. Usmani SE, Ulici V, Pest MA, Hill TL, Welch ID, Beier F. Context-specific
572 protection of TGF α null mice from osteoarthritis. *Sci Rep.* 2016 Sep 26;6(1):1–11.
573 Available from: <https://pubmed.ncbi.nlm.nih.gov/27457421/>

574 9. Loeser RF, Kelley KL, Armstrong A, Collins JA, Diekman BO, Carlson CS.
575 Deletion of JNK Enhances Senescence in Joint Tissues and Increases the
576 Severity of Age-Related Osteoarthritis in Mice. *Arthritis Rheumatol.* 2020 Oct
577 26;72(10):1679–88. Available from: <https://pubmed.ncbi.nlm.nih.gov/32418287/>

578 10. Zhang H, Wang H, Zeng C, Yan B, Ouyang J, Liu X, et al. mTORC1 activation
579 downregulates FGFR3 and PTH/PTHrP receptor in articular chondrocytes to
580 initiate osteoarthritis. *Osteoarthr Cartil.* 2017 Jun;25(6):952–63. Available from:
581 <https://pubmed.ncbi.nlm.nih.gov/28043938/>

582 11. Zhou S, Lu W, Chen L, Ge Q, Chen D, Xu Z, et al. AMPK deficiency in
583 chondrocytes accelerated the progression of instability-induced and ageing-
584 associated osteoarthritis in adult mice. *Sci Rep.* 2017 Apr 22;7(1):43245.
585 Available from: <https://pubmed.ncbi.nlm.nih.gov/28225087/>

586 12. Johnson SC, Rabinovich PS, Kaeberlein M. mTOR is a key modulator of ageing
587 and age-related disease. *Nature.* 2013;493(7432):338–45. Available from:
588 <https://pubmed.ncbi.nlm.nih.gov/23325216/>

589 13. Salminen A, Kaarniranta K, Kauppinen A. Age-related changes in AMPK
590 activation: Role for AMPK phosphatases and inhibitory phosphorylation by
591 upstream signaling pathways. *Ageing Res Rev.* 2016;28:15–26. Available from:
592 <https://pubmed.ncbi.nlm.nih.gov/27060201/>

593 14. Harrison DE, Strong R, Sharp ZD, Nelson JF, Astle CM, Flurkey K, et al.
594 Rapamycin fed late in life extends lifespan in genetically heterogeneous mice.
595 *Nature.* 2009;460(7253):392–5. Available from:
596 <https://pubmed.ncbi.nlm.nih.gov/19587680/>

597 15. Strong R, Miller RA, Antebi A, Astle CM, Bogue M, Denzel MS, et al. Longer
598 lifespan in male mice treated with a weakly estrogenic agonist, an antioxidant, an
599 α -glucosidase inhibitor or a Nrf2-inducer. *Aging Cell.* 2016 Oct 16;15(5):872–84.
600 Available from: <https://pubmed.ncbi.nlm.nih.gov/27312235/>

601 16. Barzilai N, Crandall JP, Kritchevsky SB, Espeland MA. Metformin as a Tool to
602 Target Aging. *Cell Metab.* 2016;23(6):1060–5. Available from:
603 <http://dx.doi.org/10.1016/j.cmet.2016.05.011>

604 17. Lamming DW, Ye L, Katajisto P, Goncalves MD, Saitoh M, Stevens DM, et al.
605 Rapamycin-Induced Insulin Resistance Is Mediated by mTORC2 Loss and
606 Uncoupled from Longevity. *Science* (80-). 2012 Mar 30;335(6076):1638–43.
607 Available from: <https://pubmed.ncbi.nlm.nih.gov/22461615/>

608 18. Caramés B, Hasegawa A, Taniguchi N, Miyaki S, Blanco FJ, Lotz M. Autophagy
609 activation by rapamycin reduces severity of experimental osteoarthritis. *Ann*
610 *Rheum Dis.* 2012 Apr 4;71(4):575–81. Available from:
611 <https://pubmed.ncbi.nlm.nih.gov/22084394/>

612 19. Takayama K, Kawakami Y, Kobayashi M, Greco N, Cummins JH, Matsushita T, et

613 al. Local intra-articular injection of rapamycin delays articular cartilage
614 degeneration in a murine model of osteoarthritis. *Arthritis Res Ther.* 2014 Dec
615 17;16(6):482. Available from: <https://pubmed.ncbi.nlm.nih.gov/25403236/>

616 20. Cheng N-T, Guo A, Cui Y-P. Intra-articular injection of Torin 1 reduces
617 degeneration of articular cartilage in a rabbit osteoarthritis model. *Bone Joint Res.*
618 2016 Jun;5(6):218–24. Available from:
619 <https://pubmed.ncbi.nlm.nih.gov/27301478/>

620 21. Zhang Y, Vasheghani F, Li Y, Blati M, Simeone K, Fahmi H, et al. Cartilage-
621 specific deletion of mTOR upregulates autophagy and protects mice from
622 osteoarthritis. *Ann Rheum Dis.* 2015 Jul;74(7):1432–40. Available from:
623 <https://pubmed.ncbi.nlm.nih.gov/24651621/>

624 22. Chen J, Crawford R, Xiao Y. Vertical inhibition of the PI3K/Akt/mTOR pathway for
625 the treatment of osteoarthritis. *J Cell Biochem.* 2013;114(2):245–9.

626 23. Pal B, Endisha H, Zhang Y, Kapoor M. mTOR: A potential therapeutic target in
627 osteoarthritis? *Drugs R D.* 2015;15(1):27–36. Available from:
628 <https://pubmed.ncbi.nlm.nih.gov/25688060/>

629 24. Chen K, Lin ZW, He S mao, Wang C qiang, Yang J cheng, Lu Y, et al. Metformin
630 inhibits the proliferation of rheumatoid arthritis fibroblast-like synoviocytes through
631 IGF-IR/PI3K/AKT/m-TOR pathway. *Biomed Pharmacother.* 2019;115(April
632 2018):1–8. Available from: <https://pubmed.ncbi.nlm.nih.gov/31028998/>

633 25. Wang C, Yang Y, Zhang Y, Liu J, Yao Z, Zhang C. Protective effects of metformin
634 against osteoarthritis through upregulation of SIRT3-mediated PINK1/Parkin-
635 dependent mitophagy in primary chondrocytes. *Biosci Trends.* 2018 Dec
636 31;12(6):605–12. Available from: <https://pubmed.ncbi.nlm.nih.gov/30584213/>

637 26. Petrusson F, Husa M, June R, Lotz M, Terkeltaub R, Liu-Bryan R. Linked
638 decreases in liver kinase B1 and AMP-activated protein kinase activity modulate
639 matrix catabolic responses to biomechanical injury in chondrocytes. *Arthritis Res
640 Ther.* 2013;15(4):R77. Available from: <https://pubmed.ncbi.nlm.nih.gov/23883619/>

641 27. Li J, Zhang B, Liu W-X, Lu K, Pan H, Wang T, et al. Metformin limits osteoarthritis
642 development and progression through activation of AMPK signalling. *Ann Rheum
643 Dis.* 2020 May;79(5):635–45. Available from:
644 <https://pubmed.ncbi.nlm.nih.gov/32156705/>

645 28. Wang Y, Hussain SM, Wluka AE, Lim YZ, Abram F, Pelletier J-P, et al.
646 Association between metformin use and disease progression in obese people
647 with knee osteoarthritis: data from the Osteoarthritis Initiative—a prospective
648 cohort study. *Arthritis Res Ther.* 2019 Dec 24;21(1):127. Available from:
649 <https://pubmed.ncbi.nlm.nih.gov/31126352/>

650 29. Bendele AM, Hulman JF. Effects of Body Weight Restriction on the Development
651 and Progression of Spontaneous Osteoarthritis in Guinea Pigs. *Arthritis Rheum.*
652 1991 Oct 7;34(9):1180–4. Available from:
653 <https://pubmed.ncbi.nlm.nih.gov/1930336/>

654 30. Bendele AM, White SL, Hulman JF. Osteoarthrosis in guinea pigs: histopathologic
655 and scanning electron microscopic features. *Lab Anim Sci.* 1989;39(2):115–21.
656 Available from: <https://pubmed.ncbi.nlm.nih.gov/2709799/>

657 31. Radakovich LB, Marolf AJ, Shannon JP, Pannone SC, Sherk VD, Santangelo KS.
658 Development of a microcomputed tomography scoring system to characterize

659 disease progression in the Hartley guinea pig model of spontaneous
660 osteoarthritis. *Connect Tissue Res.* 2018 Nov 2;59(6):523–33. Available from:
661 <https://pubmed.ncbi.nlm.nih.gov/29226725/>

662 32. Kraus VB, Huebner JL, DeGroot J, Bendele A. The OARSI histopathology
663 initiative - recommendations for histological assessments of osteoarthritis in the
664 guinea pig. *Osteoarthr Cartil.* 2010;18(SUPPL. 3):S35–52. Available from:
665 <http://dx.doi.org/10.1016/j.joca.2010.04.015>

666 33. Bendele AM. Animal models of osteoarthritis. In: *Journal of Musculoskeletal*
667 *Neuron Interaction.* 2001. p. 363–76. Available from:
668 <https://pubmed.ncbi.nlm.nih.gov/15758487/>

669 34. Radakovich LB, Marolf AJ, Culver LA, Santangelo KS. Calorie restriction with
670 regular chow, but not a high-fat diet, delays onset of spontaneous osteoarthritis in
671 the Hartley guinea pig model. *Arthritis Res Ther.* 2019 Dec 13;21(1):145.
672 Available from: <https://pubmed.ncbi.nlm.nih.gov/31196172/>

673 35. Martin-Montalvo A, Mercken EM, Mitchell SJ, Palacios HH, Mote PL, Scheibye-
674 Knudsen M, et al. Metformin improves healthspan and lifespan in mice. *Nat*
675 *Commun.* 2013 Oct 16;4(1):2192. Available from:
676 <https://pubmed.ncbi.nlm.nih.gov/23900241/>

677 36. Miller RA, Harrison DE, Astle CM, Baur JA, Boyd AR, de Cabo R, et al.
678 Rapamycin, But Not Resveratrol or Simvastatin, Extends Life Span of Genetically
679 Heterogeneous Mice. *Journals Gerontol Ser A.* 2011 Feb;66A(2):191–201.
680 Available from: <https://pubmed.ncbi.nlm.nih.gov/20974732/>

681 37. Weiss R, Fernandez E, Liu Y, Strong R, Salmon AB. Metformin reduces glucose
682 intolerance caused by rapamycin treatment in genetically heterogeneous female
683 mice. *Aging (Albany NY).* 2018 Mar 22;10(3):386–401. Available from:
684 <https://pubmed.ncbi.nlm.nih.gov/29579736/>

685 38. De Oliveira MA, Martins E, Martins F, Wang Q, Sonis S, Demetri G, George S, et
686 al. Clinical presentation and management of mTOR inhibitor-associated
687 stomatitis. *Oral Oncol.* 2011;47(10):998–1003. Available from:
688 <https://pubmed.ncbi.nlm.nih.gov/21890398/>

689 39. Wilkinson JE, Burmeister L, Brooks S V., Chan C-C, Friedline S, Harrison DE, et
690 al. Rapamycin slows aging in mice. *Aging Cell.* 2012 Aug;11(4):675–82. Available
691 from: <http://doi.wiley.com/10.1111/j.1474-9726.2012.00832.x>

692 40. Fraser KW. Effect of storage in formalin on organ weights of rabbits. *New Zeal J*
693 *Zool.* 1985;12(2):169–74.

694 41. Tardif S, Ross C, Bergman P, Fernandez E, Javors M, Salmon A, et al. Testing
695 Efficacy of Administration of the Antiaging Drug Rapamycin in a Nonhuman
696 Primate, the Common Marmoset. *Journals Gerontol Ser A Biol Sci Med Sci.* 2015
697 May;70(5):577–88. Available from: <https://pubmed.ncbi.nlm.nih.gov/25038772/>

698 42. Fernandez E, Ross C, Liang H, Javors M, Tardif S, Salmon AB. Evaluation of the
699 pharmacokinetics of metformin and acarbose in the common marmoset. *Pathobiol*
700 *Aging Age-related Dis.* 2019;9(1):1657756. Available from:
701 <https://pubmed.ncbi.nlm.nih.gov/31497263/>

702 43. Buie HR, Campbell GM, Klinck RJ, MacNeil JA, Boyd SK. Automatic
703 segmentation of cortical and trabecular compartments based on a dual threshold
704 technique for in vivo micro-CT bone analysis. *Bone.* 2007 Oct;41(4):505–15.

705 Available from: <https://pubmed.ncbi.nlm.nih.gov/17693147/>

706 44. Li Y, Yang J, Liu Y, Yan X, Zhang Q, Chen J, et al. Inhibition of mTORC1 in the
707 rat condyle subchondral bone aggravates osteoarthritis induced by the overly
708 forward extension of the mandible. *Am J Transl Res.* 2021;13(1):270–85.
709 Available from: <https://pubmed.ncbi.nlm.nih.gov/33527023/>

710 45. Xie J, Lin J, Wei M, Teng Y, He Q, Yang G, et al. Sustained Akt signaling in
711 articular chondrocytes causes osteoarthritis via oxidative stress-induced
712 senescence in mice. *Bone Res.* 2019 Dec 5;7(1):23. Available from:
713 <https://pubmed.ncbi.nlm.nih.gov/31646013/>

714 46. Aggarwal D, Fernandez ML, Soliman GA. Rapamycin, an mTOR inhibitor,
715 disrupts triglyceride metabolism in guinea pigs. *Metabolism.* 2006 Jun;55(6):794–
716 802. Available from: <https://pubmed.ncbi.nlm.nih.gov/16713440/>

717 47. Chen YJ, Chan DC, Lan KC, Wang CC, Chen CM, Chao SC, et al. PPAR γ is
718 involved in the hyperglycemia-induced inflammatory responses and collagen
719 degradation in human chondrocytes and diabetic mouse cartilages. *J Orthop Res.*
720 2015;33(3):373–81. Available from: <https://pubmed.ncbi.nlm.nih.gov/25410618/>

721 48. Liang H, Wang H, Luo L, Fan S, Zhou L, Liu Z, et al. Toll-like receptor 4 promotes
722 high glucose-induced catabolic and inflammatory responses in chondrocytes in an
723 NF- κ B-dependent manner. *Life Sci.* 2019;228(April):258–65. Available from:
724 <https://pubmed.ncbi.nlm.nih.gov/30953645/>

725 49. Ribeiro M, López de Figueroa P, Nogueira-Recalde U, Centeno A, Mendes AF,
726 Blanco FJ, et al. Diabetes-accelerated experimental osteoarthritis is prevented by
727 autophagy activation. *Osteoarthr Cartil.* 2016;24(12):2116–25.

728 50. Ribeiro M, López de Figueroa P, Nogueira-Recalde U, Centeno A, Mendes AF,
729 Blanco FJ, et al. Diabetes-accelerated experimental osteoarthritis is prevented by
730 autophagy activation. *Osteoarthr Cartil.* 2016;24(12):2116–25. Available from:
731 <https://pubmed.ncbi.nlm.nih.gov/27390029/>

732 51. Reifsnyder PC, Flurkey K, Te A, Harrison DE. Rapamycin treatment benefits
733 glucose metabolism in mouse models of type 2 diabetes. *Aging (Albany NY).*
734 2016;8(11):3120–30. Available from: <https://pubmed.ncbi.nlm.nih.gov/27922820/>

735 52. Watson PJ, Hall LD, Malcolm A, Tyler JA. Degenerative joint disease in the
736 guinea pig: Use of magnetic resonance imaging to monitor progression of bone
737 pathology. *Arthritis Rheum.* 1996;39(8):1327–37. Available from:
738 <https://pubmed.ncbi.nlm.nih.gov/8702441/>

739 53. Xian L, Wu X, Pang L, Lou M, Rosen C, Qui T, et al. Matrix IGF-1 regulates bone
740 mass by activation of mTOR in mesenchymal stem cells. *Nat Med.*
741 2012;18(7):1095–101. Available from: <https://pubmed.ncbi.nlm.nih.gov/22729283/>

742 54. Hamrick MW, Ding KH, Ponnala S, Ferrari SL, Isales CM. Caloric restriction
743 decreases cortical bone mass but spares trabecular bone in the mouse skeleton:
744 Implications for the regulation of bone mass by body weight. *J Bone Miner Res.*
745 2008;23(6):870–8. Available from: <https://pubmed.ncbi.nlm.nih.gov/18435579/>

746 55. Dawood AF, Alzamil N, Ebrahim HA, Abdel Kader DH, Kamar SS, Haidara MA, et
747 al. Metformin pretreatment suppresses alterations to the articular cartilage
748 ultrastructure and knee joint tissue damage secondary to type 2 diabetes mellitus
749 in rats. *Ultrastruct Pathol.* 2020;44(3):273–82. Available from:
750 <https://pubmed.ncbi.nlm.nih.gov/32404018/>

751 56. Choi YH, Sang KG, Lee MG. Dose-independent pharmacokinetics of metformin in
752 rats: Hepatic and gastrointestinal first-pass effects. *J Pharm Sci.*
753 2006;95(11):2543–52. Available from: <https://pubmed.ncbi.nlm.nih.gov/16937336/>

754 57. Graham GG, Punt J, Arora M, Day RO, Doogue MP, Duong JK, et al. Clinical
755 pharmacokinetics of metformin. *Clin Pharmacokinet.* 2011;50(2):81–98. Available
756 from: <https://pubmed.ncbi.nlm.nih.gov/21241070/>

757

758

759

760

761

762

763

764

765

766

767 **Figure Legends**

768 **Figure 1: Characterization of animals on experimental diets.** Food consumption (A)
769 and bodyweight (B) of guinea pigs were recorded for the duration of the study (data
770 presented as mean with shaded bands representing SD). Plasma glucose (C), lactate
771 (D), and testicle weight (E) are shown. **P<0.01 vs Con, ***P<0.001 vs Con, ****P<0.0001
772 vs Con.

773

774 **Figure 2: Rapamycin and rapamycin plus metformin worsened primary OA.** Representative images of histology from the medial tibia are shown for each group (A; scale bars are 0.5mm and 0.25mm in 5x and 10x images, respectively). Histological images were graded for total OARSI score (B; n=7 per group). The individual scores for articular cartilage structure (C), proteoglycan loss (D) and cellularity (E) are also shown. *P<0.05 vs Con.

780

781 **Figure 3: Proteoglycan loss correlated with hyperglycemia.** Correlations between proteoglycan loss and plasma glucose (A), bodyweight and total OARSI score (B), and testicle weight and total OARSI score (C) are shown. Shaded bands represent 95% CI.

784

785 **Figure 4: Rapamycin and rapamycin plus metformin inhibited mTORC1 but had no effect on mTORC2 or autophagy.** IHC was performed on the medial tibia for P-RPS6 (A; n=7 per group) and quantified as percent positive cells (B) and mean integrated intensity (C). Red arrowheads indicate cells staining positive for P-RPS6. Western blot was performed on glenohumeral cartilage (D) for P-RPS6 (E), P-Akt (F), P-AMPK (G), LC3B (H), ADAMTS5 (I), and MMP-13 (J). n=8 per group for Rap and n=7 per group for Con and Rap+Met. Images are outlined in black to show that, while each band is from the same blot, bands were selected for presentation to best represent the mean change. *P<0.05 vs Con, **P<0.01 vs Con.

794

795 **Figure 5: Decreased subchondral bone thickness in rapamycin and rapamycin plus metformin treated guinea pigs.** Representative microCT sagittal cross sections from the medial aspect of the joint are shown (A). Subchondral cortical thickness was measured in the medial and lateral tibial plateaus and femoral condyles (B), and cortical thickness was measured in the femoral diaphysis (C). Medial tibial cortical thickness relative to femoral diaphyseal cortical thickness was found to be similar between groups (D). Medial tibial cortical thickness was highly correlated to bodyweight (E). Femoral epicondylar width was found to be similar between groups (F). N=4 per group. Shaded bands represent 95% CI. *P<0.05 vs Con, **P<0.01 vs Con.

804 **Individual Tables and Figures**

805

806 **Table 1: Average consumption of rapamycin and metformin.** Using the concentration
807 of rapamycin and metformin from the diet analysis, the average doses were calculated
808 for each group. N=7-8 per group. Data are presented as mean \pm SD.

	Experimental Diet	
	Rapamycin	Rapamycin+Metformin
Rapamycin consumed (mg/kg/day)	0.72 \pm 0.09	0.68 \pm 0.08
Metformin consumed (mg/kg/day)	-	45 \pm 5.6

809

810

811

812

813

814

815

816

817

818

819

820

821

822

823

824

825

826

827

828

829

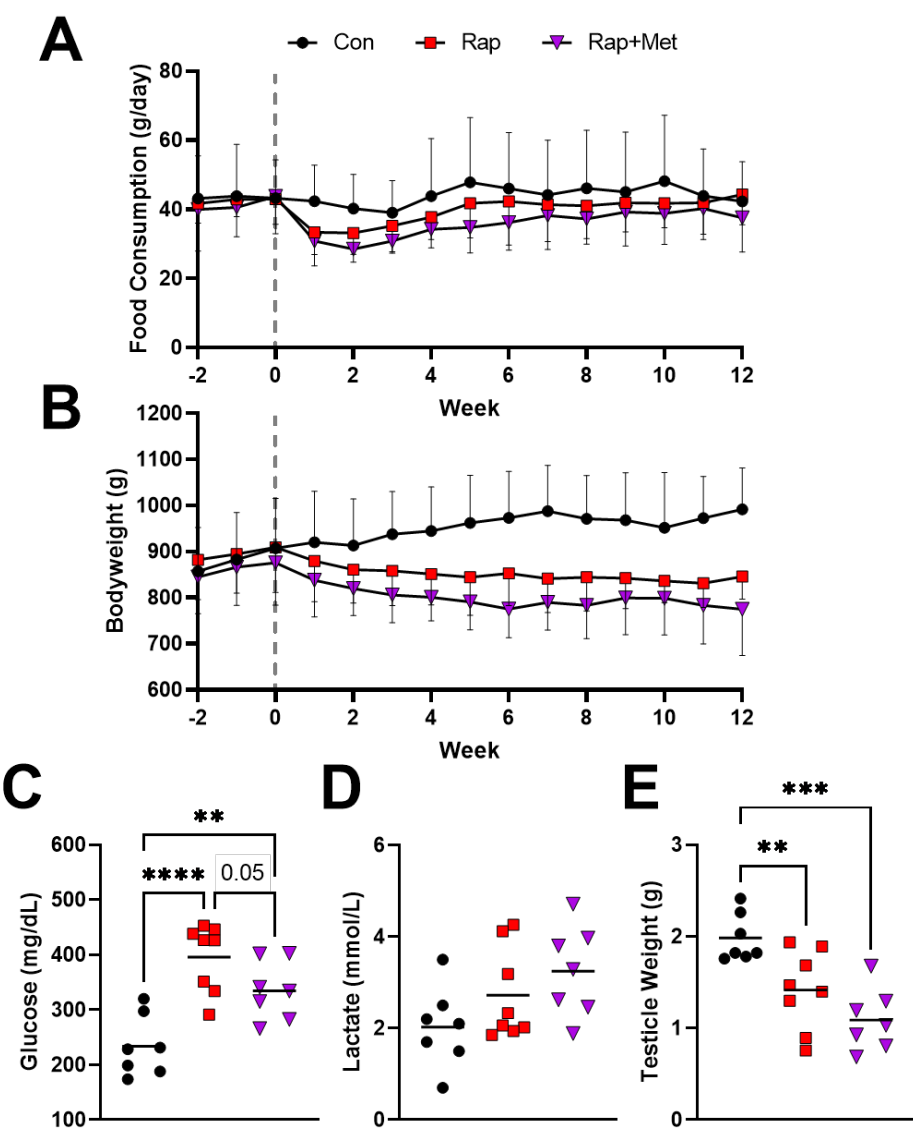
830

831 **Table 2: Concentrations of rapamycin and metformin in circulation.** Whole blood
832 was collected ~3 hours after food had been removed from the cages of guinea pigs and
833 was analyzed for rapamycin and metformin concentration by tandem HPLC/MS. N=4 per
834 group. Data are presented as mean with \pm SD.

	Experimental Diet		
	Control	Rapamycin	Rapamycin+Metformin
Circulating rapamycin (ng/mL)	0.4 \pm 0	72 \pm 8	78 \pm 10
Circulating metformin (ng/mL)	2 \pm 0	-	282 \pm 54

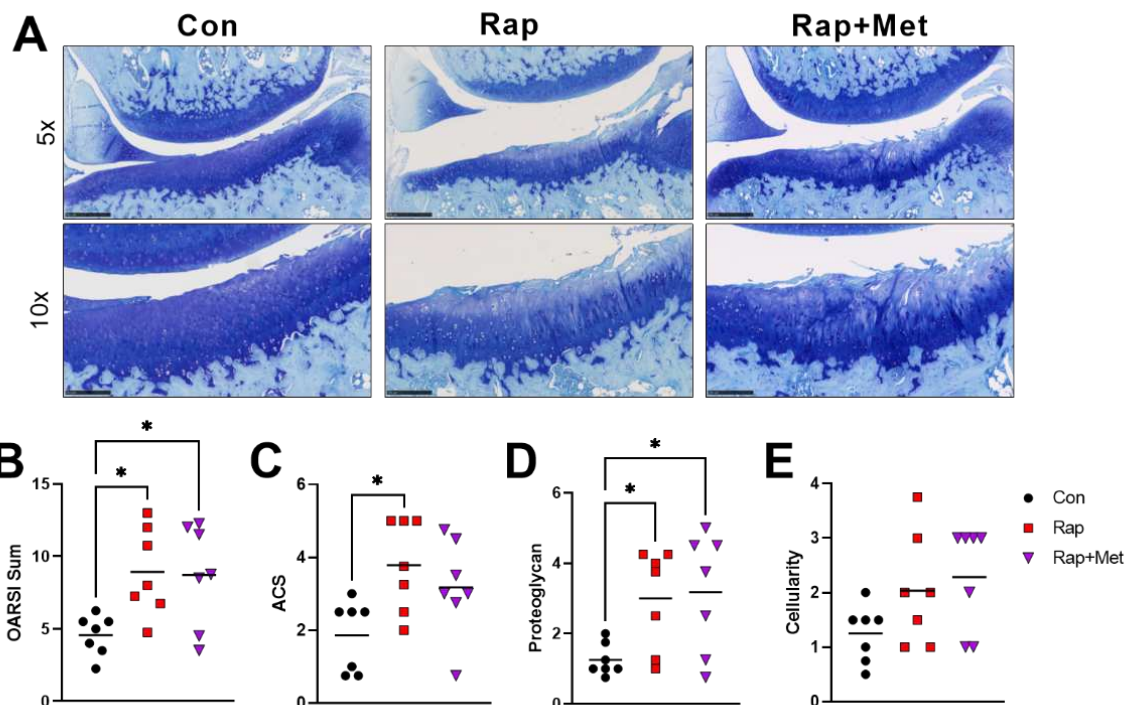
835
836
837
838
839
840
841
842
843
844
845
846
847
848
849
850
851
852
853
854
855
856
857
858
859
860
861
862
863
864

865 **Figure 1**



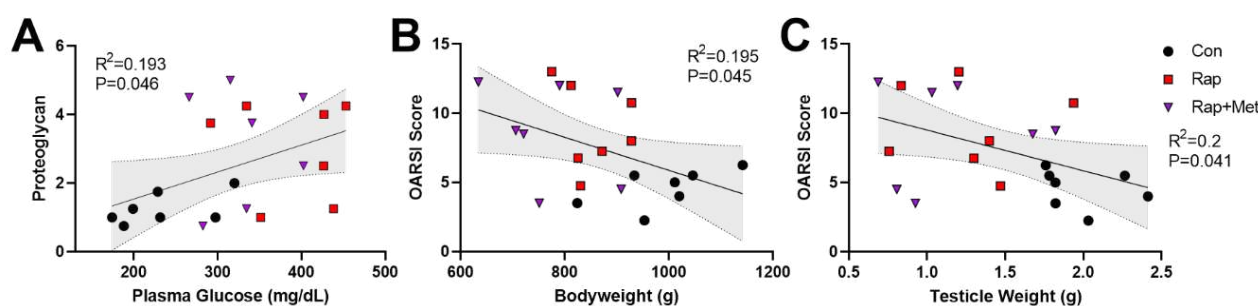
866
867
868
869
870
871
872
873
874

875 **Figure 2**
876



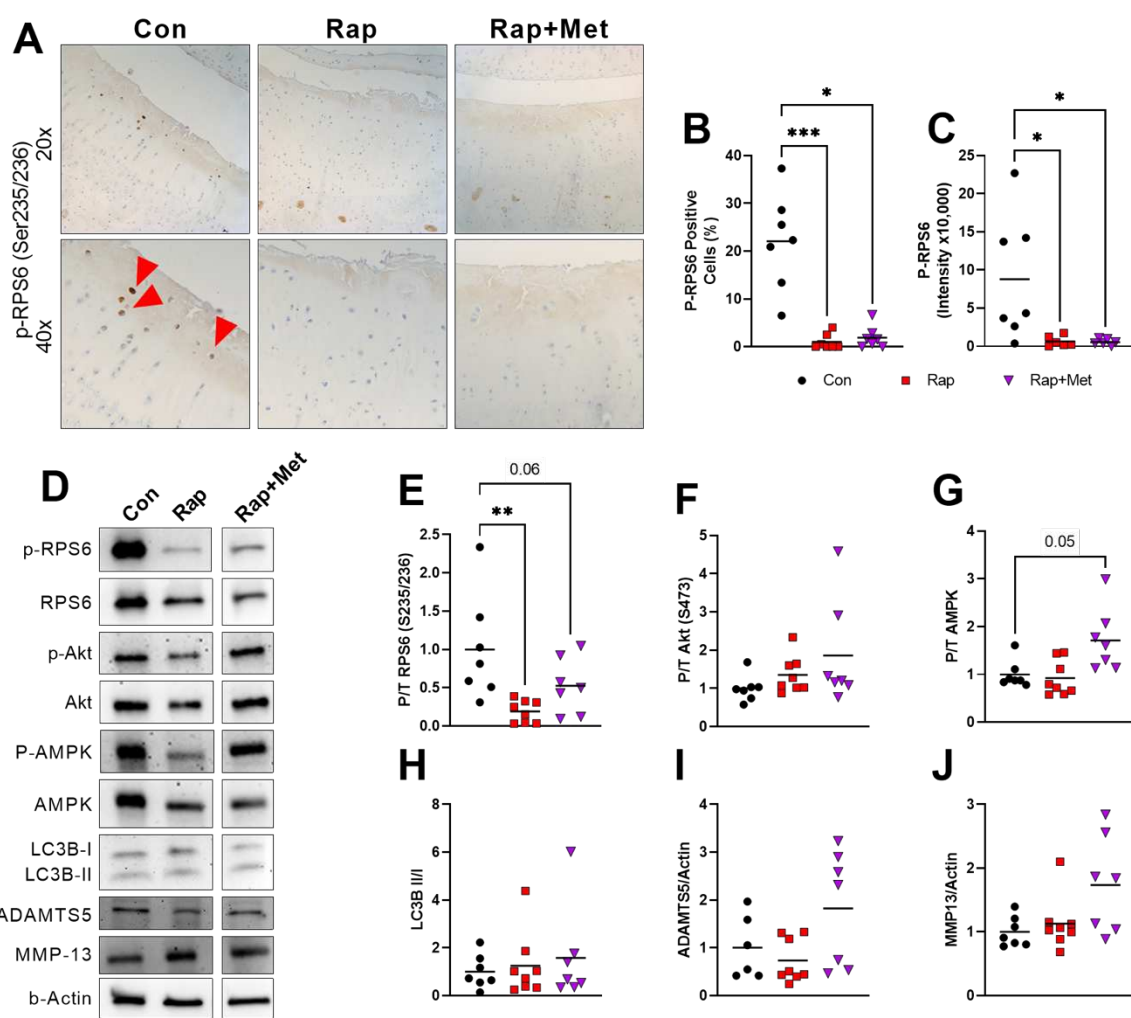
877
878
879
880
881
882
883
884
885
886
887
888
889
890
891
892

893 **Figure 3**



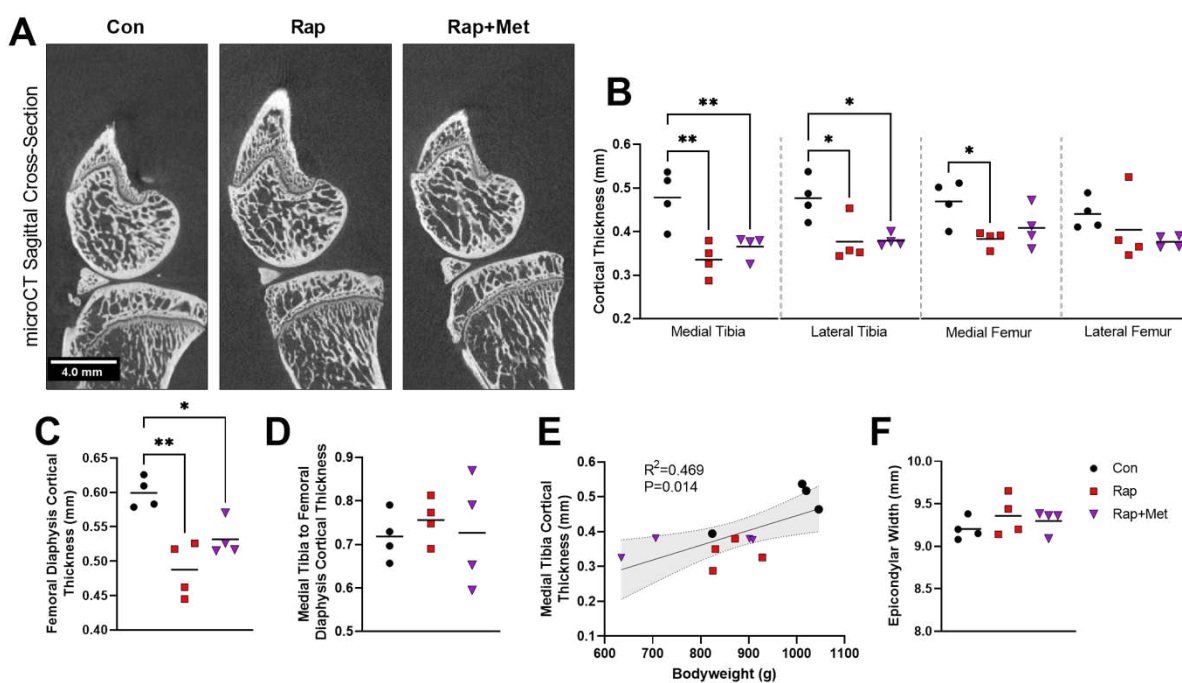
894
895
896
897
898
899
900
901
902
903
904
905
906
907
908
909
910
911
912
913
914
915
916
917
918
919
920
921
922
923
924
925
926
927
928
929

930 **Figure 4**



931
932
933
934
935
936
937
938
939
940
941
942
943
944
945
946
947
948

949 **Figure 5**



950
951
952
953
954
955
956
957
958
959
960
961
962
963
964
965
966
967
968

969
970
971

972

973 **Supplementary Material**

974 Supplementary Figure Legends

975 **Figure S1: OA pathology increased from 5- to 8-months of age.** Total OARSI scores

976 are shown from the lateral tibia, medial femur, and lateral femur (A). Histological images

977 of knee joints from 5- and 8-month-old guinea pigs (B; scale bars are 0.5mm and 0.25mm

978 in 5x and 10x images, respectively) were graded for total OARSI score and individual

979 OARSI criteria (C). N=3 for 5-month and N=7 for 8-month. *P<0.05 vs Con.

980

981 **Figure S2: Trabecular bone changes in response to experimental diets.** Trabecular

982 thickness (A), spacing (B), and bone volume fraction (C) were measured using microCT.

983 N=4 per group. *P<0.05 vs Con.

984

985 **Figure S3: Antibody reactivity with guinea pig articular cartilage was limited.**

986 Immunohistochemical staining was performed, and no reactivity was observed using

987 primary antibodies against P-Akt Ser473 or P-AMPK Thr172.

988

989

990

991

992

993

994

995

996

997

998

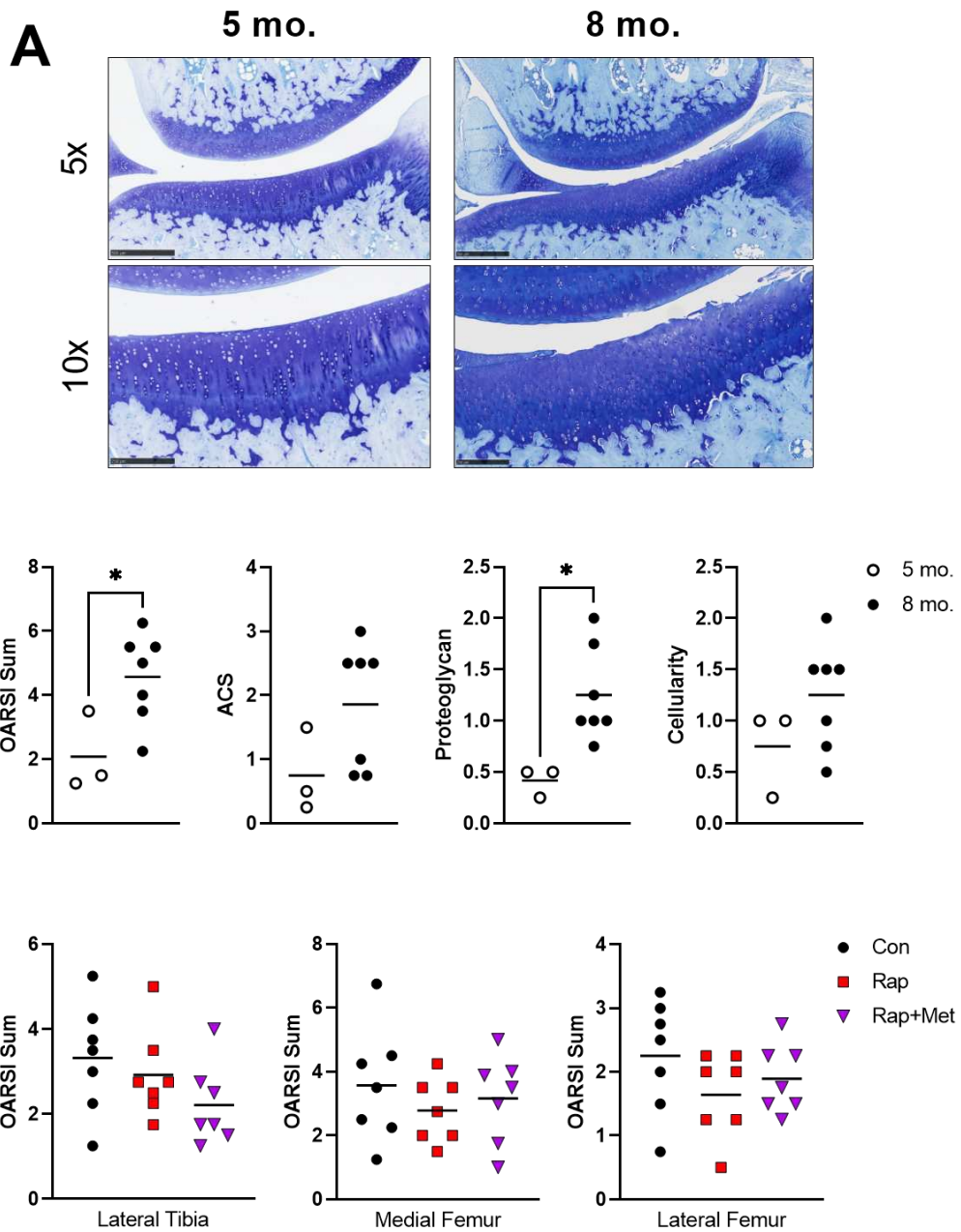
999

1000

1001

1002
1003
1004
1005

Supplementary Figures
Figure S1

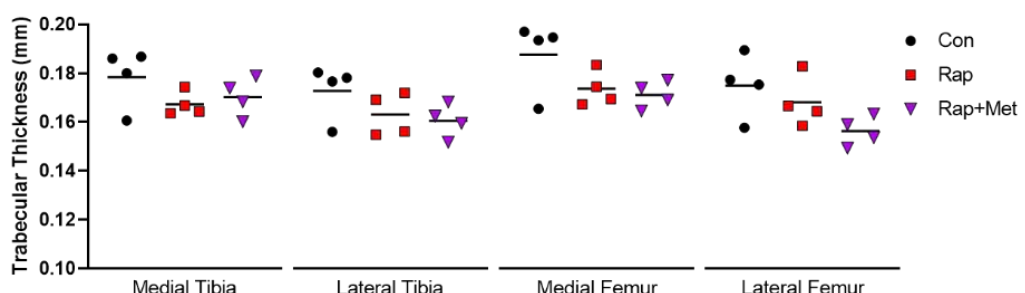


1006
1007
1008
1009
1010
1011

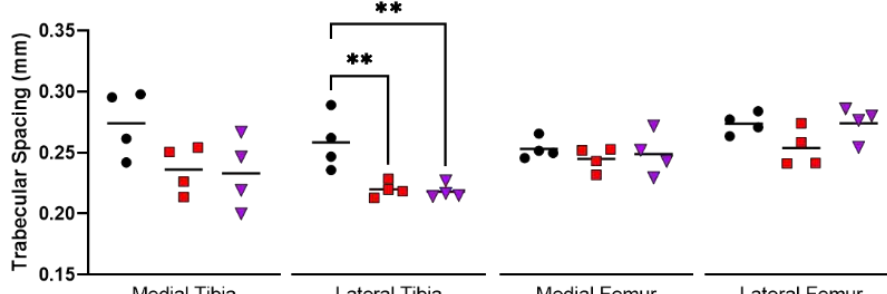
1012
1013
1014

Figure S2

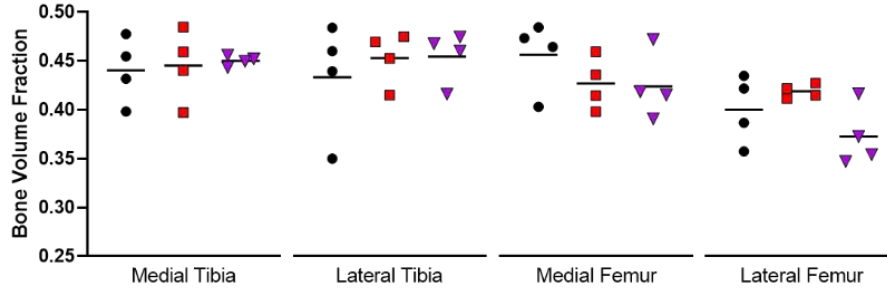
A



B



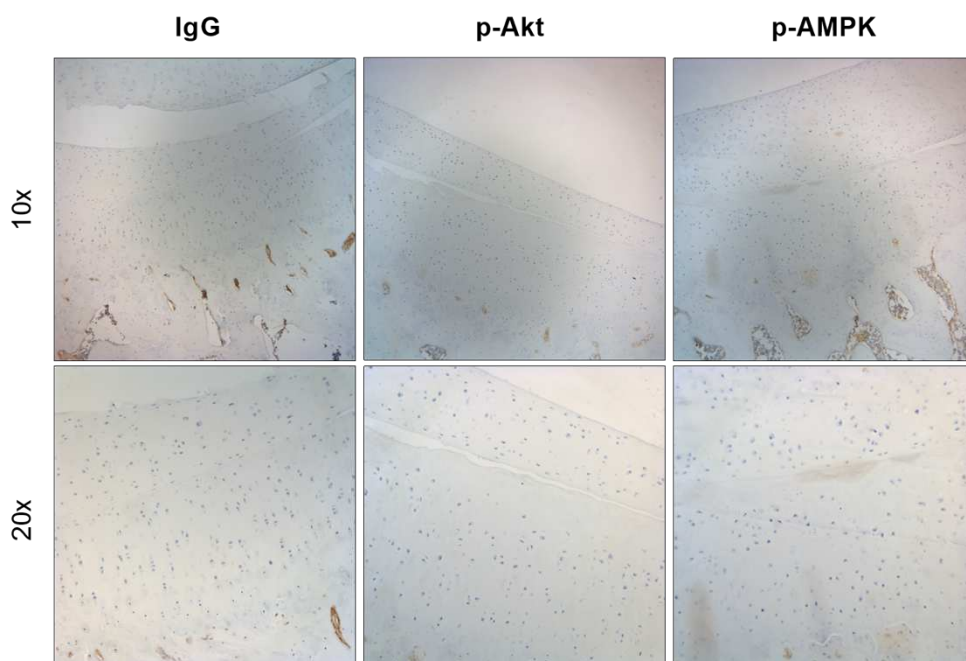
C



1015
1016
1017
1018
1019
1020
1021
1022
1023
1024
1025
1026
1027
1028

1029
1030
1031

Figure S3



1032